AFRL-RX-WP-TP-2009-4216

CONSTITUTIVE MODELING OF LOW-TEMPERATURE SUPERPLASTIC FLOW OF ULTRAFINE Ti-6AI-4V SHEET MATERIAL (PREPRINT)

S.L. Semiatin and G.A. Sargent

Metals Branch
Metals, Ceramics and NDE Division

JUNE 2009

STINFO COPY

AIR FORCE RESEARCH LABORATORY
MATERIALS AND MANUFACTURING DIRECTORATE
WRIGHT-PATTERSON AIR FORCE BASE, OH 45433-7750
AIR FORCE MATERIEL COMMAND
UNITED STATES AIR FORCE

REPORT DOCUMENTATION PAGE

The public reporting burden for this collection of information is estimated to average 1 hour per response, including the time for reviewing instructions, searching existing data sources, searching existing data sources, gathering and maintaining the data needed, and completing and reviewing the collection of information. Send comments regarding this burden estimate or any other aspect of this collection of information, including suggestions for reducing this burden, to Department of Defense, Washington Headquarters Services, Directorate for Information Operations and Reports (0704-0188), 1215 Jefferson Davis Highway, Suite 1204, Arlington, VA 22202-4302. Respondents should be aware that notwithstanding any other provision of law, no person shall be subject to any penalty for failing to comply with a collection of information if it does not display a currently valid OMB control number. **PLEASE DO NOT RETURN YOUR FORM TO THE ABOVE ADDRESS**.

1. REPORT DATE *(DD-MM-YY)*	2. REPORT TYPE	3. DATES COVERED *(From - To)*
June 2009	Journal Article Preprint	01 June 2009 – 01 June 2009

4. TITLE AND SUBTITLE	5a. CONTRACT NUMBER
CONSTITUTIVE MODELING OF LOW-TEMPERATURE SUPERPLASTIC FLOW OF UNLTRAFINE Ti-6AI-4V SHEET MATERIAL (PREPRINT)	In-house
	5b. GRANT NUMBER
	5c. PROGRAM ELEMENT NUMBER 62102F

6. AUTHOR(S)	5d. PROJECT NUMBER 4347
S.L. Semiatin (AFRL/RXLMP)	5e. TASK NUMBER RG
G.A. Sargent (UES, Inc.)	5f. WORK UNIT NUMBER M02R2000

7. PERFORMING ORGANIZATION NAME(S) AND ADDRESS(ES)		8. PERFORMING ORGANIZATION REPORT NUMBER
Metals Branch (RXLMN) Metals, Ceramics and NDE Division Materials and Manufacturing Directorate Wright-Patterson Air Force Base, OH 45433-7750 Air Force Materiel Command, United States Air Force	UES, Inc. 4401 Dayton-Xenia Road Dayton, OH 45432	AFRL-RX-WP-TP-2009-4216

9. SPONSORING/MONITORING AGENCY NAME(S) AND ADDRESS(ES)	10. SPONSORING/MONITORING AGENCY ACRONYM(S)
Air Force Research Laboratory Materials and Manufacturing Directorate Wright-Patterson Air Force Base, OH 45433-7750 Air Force Materiel Command United States Air Force	AFRL/RXLMP
	11. SPONSORING/MONITORING AGENCY REPORT NUMBER(S) AFRL-RX-WP-TP-2009-4216

12. DISTRIBUTION/AVAILABILITY STATEMENT
Approved for public release; distribution unlimited.

14. ABSTRACT
The low-temperature superplastic flow behavior of two lots of Ti-6Al-4V sheet with an ultrafine microstructure was modeled. One lot (Sheet A) had an equiaxed-alpha starting microstructure; the flow stress/flow hardening exhibited by this material was explained on the basis of the Bird-Mukherjee-Dorn constitutive equation. The other material (Sheet B), having a mixed equiaxed- and remnant-lamellar alpha microstructure, underwent flow softening, flow hardening, or steady-state flow depending on test temperature and strain rate. These behaviors were interpreted in the context of a dynamic spheroidization model. The apparent flow softening at the end of all of the flow curves was explained using a simple flow-localization model.

15. SUBJECT TERMS
low-temperature superplasticity, constitutive behavior, flow hardening, dynamic spheroidization, flow-localization analysis

16. SECURITY CLASSIFICATION OF:			17. LIMITATION OF ABSTRACT:	18. NUMBER OF PAGES	19a. NAME OF RESPONSIBLE PERSON (Monitor)
a. REPORT Unclassified	b. ABSTRACT Unclassified	c. THIS PAGE Unclassified	SAR	12	Sheldon L. Semiatin 19b. TELEPHONE NUMBER *(Include Area Code)* N/A

Constitutive Modeling of Low-Temperature Superplastic Flow of Ultrafine Ti-6Al-4V Sheet Material

S.L. Semiatin[1, a] and G.A. Sargent[2,b]

[1]Air Force Research Laboratory, Materials and Manufacturing Directorate,
AFRL/RXLM, Wright-Patterson Air Force Base, OH 45433-7817 USA

[2]UES, Inc., 4401 Dayton-Xenia Road, Dayton, OH 45432 USA

[a]lee.semiatin@wpafb.af.mil, [b]gordon.sargent@wpafb.af.mil

Keywords: Low-temperature superplasticity, constitutive behavior, flow hardening, dynamic spheroidization, flow-localization analysis.

Abstract. The low-temperature superplastic flow behavior of two lots of Ti-6Al-4V sheet with an ultrafine microstructure was modeled. One lot (Sheet A) had an equiaxed-alpha starting microstructure; the flow stress/flow hardening exhibited by this material was explained on the basis of the Bird-Mukherjee-Dorn constitutive equation. The other material (Sheet B), having a mixed equiaxed- and remnant-lamellar alpha microstructure, underwent flow softening, flow hardening, or steady-state flow depending on test temperature and strain rate. These behaviors were interpreted in the context of a dynamic spheroidization model. The apparent flow softening at the end of all of the flow curves was explained using a simple flow-localization model.

Introduction

The development of novel deformation, solidification, and vapor processes to impart ultrafine microstructure has spurred great interest in the superplastic behavior of metallic materials at low temperatures and/or high strain rates. Much of this work has focused on nominally single-phase or particle-containing alloys such as those based on aluminum. By comparison, relatively little work has been done in this area for two-phase alloys for which processing is much more challenging. One such class of materials comprises alpha/beta titanium alloys. Low-temperature superplastic sheet forming or isothermal forging of titanium could lead to reduced tooling cost, faster cycle times, and better material utilization [1].

Recent work for a prototypical alpha/beta titanium alloy (Ti-6Al-4V) has shown that an ultrafine microstructure can be developed in billet and sheet products via severe-plastic-deformation processes such as rolling, multi-axial ('abc') forging, equal-channel-angular extrusion, or high-pressure torsion at warm-working temperatures [2-5]. Values of the strain-rate sensitivity of the flow stress of the order of 0.35 to 0.65 and elongations in excess of 400 pct. have been obtained by these means at low temperatures (~700-800°C) and strain rates typical of conventional superplastic forming (~10^{-3} s^{-1}). However, the measured stress-strain response (e.g., flow-hardening, flow-softening, or steady-state flow) has varied from one investigation to the next [1, 4, 6-8].

The objective of the present work was to establish and interpret the source of differences in the constitutive response of Ti-6Al-4V sheet with an ultrafine microstructure. For this purpose, the uniaxial-tension flow curves of two lots of this material were analyzed in terms of overall constitutive behavior, measured flow hardening/flow softening rates, and quasi-stable flow/plastic instability at large strains. These results were also compared to related plastic-flow observations determined in compression for a Ti-6Al-4V billet product with an ultrafine microstructure [9].

Materials and Procedures

Two different lots of Ti-6Al-4V sheet of ~2-mm thickness, denoted as Sheet A and Sheet B, were used to quantify the constitutive response of a typical alpha/beta titanium alloy with an ultrafine microstructure. Produced using proprietary methods by VSMPO (Russia) and supplied by Boeing

Commercial Airplane Company, the two materials had essentially identical compositions (well within the specification for this material) but different microstructures (Fig. 1). Sheet A had a microstructure of ~2-μm equiaxed-alpha particles in a matrix of beta, whereas Sheet B had a mixed microstructure of elongated (~3-μm thick, aspect ratio of ~2:1) and equiaxed-alpha particles.

Uniaxial-tension tests were conducted in a vacuum furnace at temperatures of 775 and 815°C and constant true (axial) strain rates of 10^{-4} or 10^{-3} s^{-1} to determine stress-strain behavior. Samples were preheated for 15 minutes (or, in selected cases, for 60 minutes) prior to tension testing. Because of a stroke limitation for the test system, the samples could only be taken to a total elongation of ~700 pct. which was shy of failure in all cases. Load-stroke data were reduced to true stress-true strain by taking the machine compliance into account and assuming uniform deformation even after the onset of diffuse necking. In addition, selected strain-rate jump tests were conducted to determine the strain-rate sensitivity of the flow stress (m value) as function of true strain. Post-testing metallography via backscatter-electron-imaging in a scanning-electron microscope was used to establish the final microstructure along the gage length of each sample.

The measured flow stresses and flow-hardening behaviors for Sheet A were interpreted in the context of the Bird-Mukherjee-Dorn phenomenological constitutive relation [10]. Observations of flow softening (for Sheet B) were analyzed in terms of diffusion-controlled *dynamic* spheroidization kinetics. The suitability of the assumption of uniform flow used to reduce the load-stroke data was analyzed using a long-wavelength flow-localization model. Such modeling was based on a simple load-equilibrium approach [11] using various degrees of sample discretization (i.e., 3, 6, or 11 slices for half of the specimen) and two sizes of an initial geometric defect, i.e., $f_o = 0.98$ or 0.99.
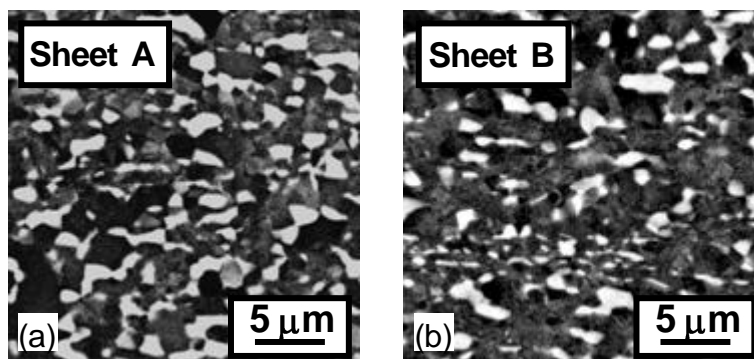

Fig. 1. Microstructures of Ti-6Al-4V program alloys following heat treatment at 775°C/15 min + water quenching: (a) Sheet A, (b) Sheet B.

Results and Discussion

The principal findings of this research comprise the measurement and interpretation of stress-strain response, flow hardening/flow softening, and plastic instability.

Stress-Strain Response. The stress-strain response observed for Sheets A and B showed some similarities and some differences (e.g., Fig. 2 illustrating results for samples *preheated 15 minutes* prior to tension testing). All of the flow curves for Sheet A (Fig. 2a) revealed relatively low flow stresses and flow hardening except at large strains. Qualitatively similar behavior was noted for Sheet B tested at 10^{-4} s^{-1}. However, this material showed substantially higher initial stresses followed by flow softening or near-steady-state flow at 10^{-3} s^{-1} and both test temperatures (Fig. 2b).

There was little effect of preheat time (i.e., 15 vs. 60 minutes) on the stress-strain behavior of both sheet materials when tested at 10^{-4} s^{-1}. This was as expected in view of the fact that the duration of the tensile deformation itself (and the associated metallurgical processes) greatly exceeded either preheat time at this strain rate. In addition, the results for Sheet B at 10^{-3} s^{-1} were similar irrespective of preheat time (Fig. 3a); it can thus be concluded that preheat time had little influence on the microstructure of Sheet B (*containing remnant alpha lamellae*) prior to deformation at this strain rate. On the other hand, the limited 10^{-3} s^{-1}, 60-minute preheat results for Sheet A revealed higher initial flow stresses and less flow hardening than the corresponding results for samples preheated only 15 minutes. This preheat-time dependence was similar to previous observations for a Ti-6Al-4V billet with an ultrafine *equiaxed-alpha* microstructure (Fig. 3b [9])

and has been determined to be a result of a large amount of static coarsening during long preheat times prior to deformation.

Both materials exhibited relatively high values of the strain-rate sensitivity of the flow stress for all test conditions (i.e., between ~0.6 and 0.75) over the entire range of strains between 0 and 1.5. The values of m tended to show a small decrease with increasing strain, however.
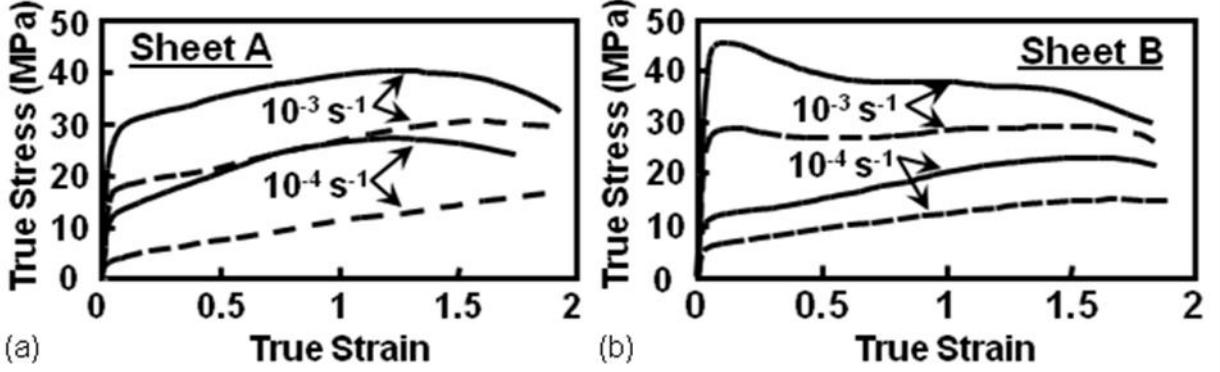

Fig. 2. True stress-true strain curves obtained at 775°C (solid lines) or 815°C (broken lines) for (a) Sheet A and (b) Sheet B. Preheat time prior to tension testing was 15 minutes in all cases.
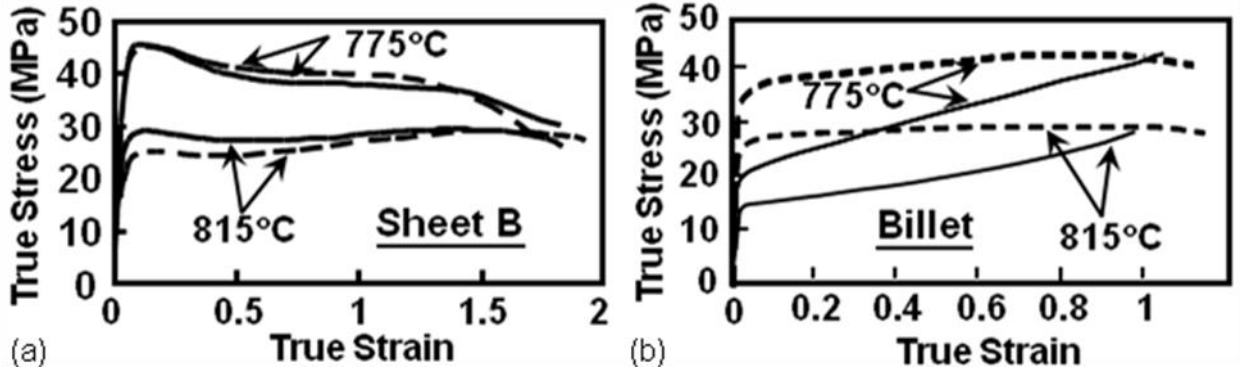

Fig. 3. True stress-true strain curves obtained after a preheat of 15 mutes (solid lines) or 60 minutes (broken lines) and a strain rate of 10^{-3} s^{-1} for (a) Sheet B or (b) an ultrafine Ti-6Al-4V billet material. The billet-material data are compression results in the literature [9].

Constitutive Behavior and Flow Hardening – Sheet A. The magnitude of the flow stress σ and the flow-hardening rates of Sheet A were successfully modeled using the Bird-Mukherjee-Dorn generalized constitutive relation, often applied for superplastic flow of *single-phase* materials [10]:

$$\dot{\varepsilon} = (\frac{ADGb}{kT})(\frac{\sigma}{G})^{n} (\frac{b}{d})^{p} .$$

(1)

Here, $\dot{\varepsilon}$ denotes the applied strain rate, A is a constant (~10), D is a diffusivity pertinent to the dynamic process which limits the rate at which strain concentrations due to grain-boundary/interface sliding are relaxed, G = the shear modulus, k = Boltzmann's constant, b = length of the Burgers vector, T = test temperature, d = the grain diameter, n (=1/m) is the stress exponent of the strain rate, and p is the grain-size exponent of the strain rate. For *two-phase* alloys such as Ti-6Al-4V, the meaning of these terms becomes unclear. Recent work for an ultrafine Ti-6Al-4V billet material tested in compression [9] has suggested that superplastic deformation occurs by sliding along the interface between alpha particles and the surrounding beta matrix with stress concentrations accommodated by deformation of the beta phase. In this sense, the alpha particles act like the core and the beta matrix as the mantle in the classical Gifkins model of superplastic flow of single-phase alloys [12]. Thus, the quantities D, G, and b refer to the beta matrix, and d is the alpha-particle diameter for alpha/beta titanium alloys. As was done previously for the compression data obtained for the ultrafine Ti-6Al-4V billet product, the correctness of this hypothesis was demonstrated by re-arranging Eq. 1 and plotting the calculated values of AD versus 1/T for Sheet A

data (at the beginning and end of the tension tests) and Sheet B data (only at the end of the tests at which the alpha particles had become spheroidized) (Fig. 4). In making this graph, the grain size exponent p was taken to be 2 (per previous work [9]), and n was assumed to be 1.67 (i.e., m = 0.6). The experimental points from the tension tests were found to lie close to the trend line for the previous compression results, thus suggesting a unique constitutive behavior irrespective of whether deformation is imposed in tension or compression. Furthermore, the fact that all of the plastic-flow results lie at values of AD approximately one order of magnitude higher than D_V^β suggests that A ≈ 10 for the superplastic flow of ultrafine Ti-6Al-4V. Such an increase in the dynamic diffusivity (i.e., 'AD') is comparable to the enhancement of coarsening due to concurrent deformation [9].

The flow hardening observed during Sheet A tension tests (Fig. 2a) was modeled by coupling the generalized constitutive equation (in the *normalized* form $\sigma/\sigma_o = (d/d_o)^{p/n}$) with the phenomenological relation describing dynamic coarsening of the alpha particles (of average *radius* $\bar{r}_\alpha$) as a function of time t (or, equivalently, imposed axial strain $\varepsilon = \dot{\varepsilon}\,t$):

$$\bar{r}_\alpha^3 - \bar{r}_{\alpha o}^3 = K_d(t - t_o) = (K_d/\dot{\varepsilon})(\varepsilon - \varepsilon_o)\,. \qquad (2)$$

The subscript 'o' indicates quantities at some specified initial time, and K_d denotes the dynamic-coarsening rate constant. The values of K_d ($\mu m^3/h$) were measured previously [13]: 3.9 (775°C, 10^{-4} s^{-1}), 8.8 (775°C, 10^{-3} s^{-1}), 6.8 (815°C, 10^{-4} s^{-1}), and 15.8 (815°C, 10^{-3} s^{-1}). Taking p = 2 and values of m (=1/n) that bound the measurements (0.6 and 0.75), predicted (normalized) flow curves were obtained and showed reasonable agreement with the Sheet A measurements (Fig. 5).
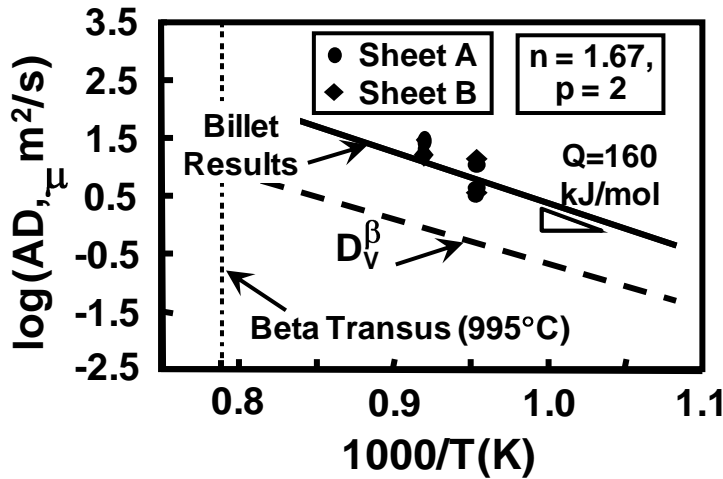

Figure 4. Plot of AD vs 1/T for tension flow stress data obtained on Sheet A (at the beginning and end of deformation, closed circles) and Sheet B (end of deformation only, closed diamonds). The data points are compared to trend lines describing results from hot compression tests on an ultrafine Ti-6Al-4V billet material and the diffusivity of vanadium in beta titanium (D_V^β) [9].
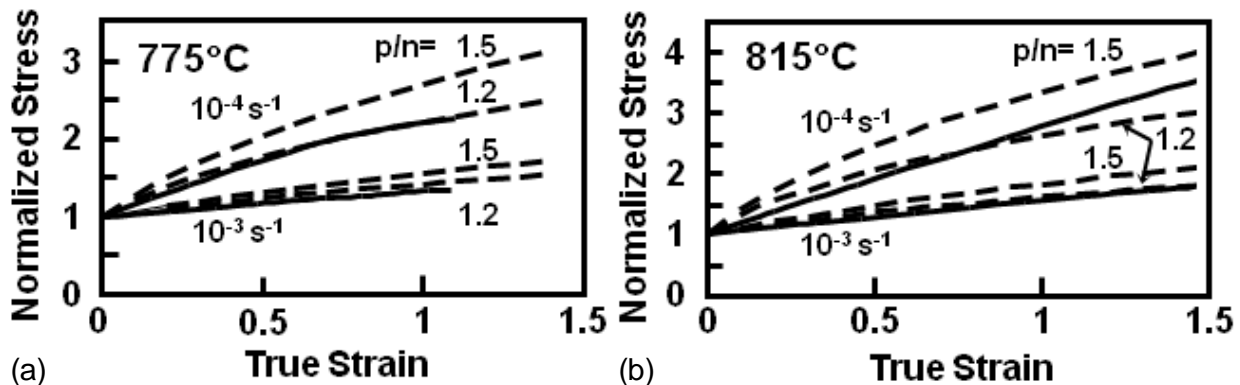

Fig. 5. Comparison of measured normalized flow curves for Sheet A (solid lines) and predictions based on the generalized constitutive and coarsening equations (broken lines): (a) 775°C and (b) 815°C.

Flow Behavior – Sheet B. Periods of flow softening and steady-state flow observed for Sheet B (Fig. 2b) were deduced to be related to dynamic spheroidization of remnant lamellae. Such a process in essence reduces the effective diameter of the lamellae resulting in softening which counterbalances flow hardening due to dynamic coarsening. Semi-quantitative insight into the time

for and relative rates of *dynamic* spheroidization were obtained from a previous analysis of the time τ_{vd} for *static* spheroidization of a pancake-shaped particle of diameter w and thickness u [14], viz.,

$$\frac{\tau_{vd}}{\tau'} = \frac{\eta^3 - [0.328\eta^{7/3}\left(1+\sqrt{1-0.763\eta^{-4/3}}\right)^2]}{4[\dfrac{2(1+\eta)}{3(0.5-0.573\eta^{-1/3})} + \dfrac{0.5\eta^{1/3}+0.665\eta^{2/3}}{3(0.143+0.934\eta^{-1/3})}]} \quad . \tag{3}$$

In this equation, $\eta = w/u + 0.5$ (≈ 2.5 in the present work) and $\tau' = u^3 R_g T / D_\beta C_F \gamma_{\alpha\beta} V_M$, in which R_g = the gas constant, T = temperature (in K), D_β = diffusivity of the rate-limiting solute in beta titanium, C_F = a concentration factor (= 11.8 at 775°C and 15.6 at 815°C) [14], $\gamma_{\alpha\beta}$ = the alpha/beta interface energy (0.4 J/m^2), and V_M = the molar volume of the alpha-platelet material (10^{-5} m^3/mol). As noted above, D_β under dynamic (superplastic-deformation) conditions is approximately 10 times greater than the corresponding static diffusivity; thus $D_\beta \sim 0.045$ or 0.083 μm^2/s at 775 and 815°C, respectively. Inserting these values into Eq. 3 results in predicted spheroidization times of 1.53 h (5500 s) at 775°C and 0.63 h (2270 s) at 815°C. For tests at 10^{-4} s^{-1}, dynamic spheroidization at the two test temperatures would thus be complete by rather small strains (0.55 or 0.23, respectively). Therefore, the observed absence of flow softening at the lower strain rate (Fig. 2b) can be rationalized. By contrast, strains of the order of ~5 or ~2 would be required to complete dynamic spheroidization at a strain rate of 10^{-3} s^{-1} and the two different test temperatures. These strains exceed those imposed and thus can explain the observed flow softening at least qualitatively.

The analysis in Reference 14 can also be used to understand the *relative rate* of dynamic spheroidization and the qualitative shape of the 10^{-3} s^{-1} flow curves for Sheet B. Specifically, because of the cube dependence of τ' on the platelet thickness, the rate of spheroidization at the beginning would tend to be much greater than later in the process. In particular, using the equations in Table 1 of Ref. 14, the ratio of the flux (volume of material transported per unit time) at the beginning and midpoint of spheroidization (for $\eta = 2.5$) is equal to ~10. Thus, the high initial rates of flow softening in the 10^{-3} s^{-1} flow curves (Figure 2b), relative to those observed at higher strains, appears to be reasonable.

Flow-Localization-Analysis Results. Predicted stress-strain curves from the flow-localization analysis established the source of the apparent flow softening found at strains of ~1.5 – 2 in many of the flow curves (Figure 2). The analysis was simplified by noting that essentially identical microstructures were developed along the entire length of deformed tension specimens containing diffuse necks [13]. These observations led to the conclusion that the observed flow hardening (e.g., Fig. 2a for Sheet A) was not strain hardening per se but an indication of an increase in the strength coefficient C = C(t) (characterizing stress-strain behavior) due to time-dependent dynamic coarsening. Thus, a constitutive equation of the form $\sigma = C\varepsilon^n \dot{\varepsilon}^m$ was used in the flow-localization calculations. Neglecting stress triaxiality (because of the diffuseness of the neck developed in superplastic materials), the following load-equilibrium relation was used in the analysis:

$$\delta P = \delta\{\sigma_x A\} = \delta\{C(t)[(\dot{\varepsilon}/\dot{\varepsilon}_o)^m] A\} = 0, \tag{4}$$

in which δP denotes the variation in axial load along the length (x-coordinate) of the specimen, σ_x is the axial stress, $\dot{\varepsilon}_o$ is a reference strain rate, and A is the local cross-sectional area.

Typical results from the flow-localization analysis, taking C(t) = constant = 100 (in arbitrary units, A.U.), are shown in Figure 6 in terms of the predicted flow behavior calculated from the simulation load and overall sample length; this enables a direct comparison to measured flow curves obtained from load-stroke data assuming uniform deformation along the gage length. (It should be emphasized that because of the form of the constitutive equation, the choice of C = constant does not change the strain at which diffuse necking occurs [15].) Simulation results with different degrees of discretization indicated no change in predictions with six or greater slices (Fig. 6a). Model predictions from a variety of six-slice simulations did show apparent flow-softening at a strain dependent on the m value and the size of the initial geometry defect f_o (Fig. 6b). This

apparent flow softening had a shape and occurred at strains similar to the experimental results (Fig. 2). It should be borne in mind, however, that the apparent softening at large strains in Fig. 6 is *not* a material property per se but rather an artifact of the use of the uniform-deformation assumption to reduce load-stroke date even after the onset of diffuse necking. That this is indeed the case was further underscored by comparing simulation results to analytical predictions of the "limit strain" ε_f from a long-wavelength *two-slice* flow-localization model. i.e., $\varepsilon_f = (-m)\{\ln(1- f_o^{1/m})\}$ [15]. These latter predictions for the various values of m and f_o, shown by the solid circles in Fig. 6b, do fall on the flow curves at the points at which the *apparent* softening starts to become significant.
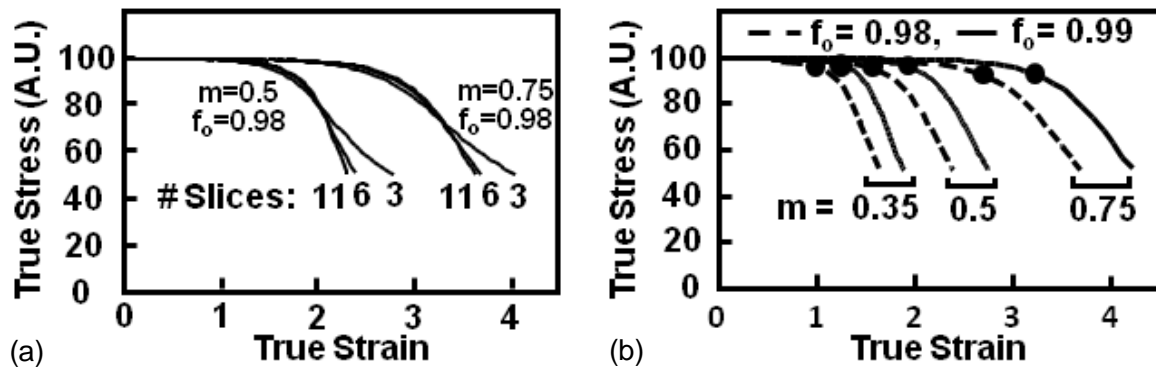

Fig. 6. Flow-localization-model predictions showing the effect of (a) number of specimen slices and (b) values of m and f_o on stress-strain behavior. The solid circes in (b) are predicted limit strains from an analytical two-slice, long-wavelength model [15].

Summary

Various features of the superplastic flow of ultrafine Ti-6Al-4V sheet were successfully interpreted using (a) a phenomenological generalized constitutive equation (flow stress levels, flow hardening), (b) a model for dynamic spheroidization (flow softening at low strains), and (c) a flow-localization analysis (apparent flow softening at large strains, an artifact of the application of the uniform-deformation assumption during diffuse necking).

References

[1]   P. N.Comley: J. Mater. Eng. Perf. Vol. 13 (2004), p. 660.
[2]   H. Inagaki: Z. fur Metallkunde Vol. 86 (1995), p. 643.
[3]   G.A. Salishchev, et al.: J. Mater. Proc. Techn. Vol 116 (2001), p. 265.
[4]   Y.G. Ko, et al.: Metall. Mater. Trans. A Vol. 37A (2006), p. 381.
[5]   A.V. Sergueeva, et al.: Mater. Sci. Eng. A Vol. A323 (2002), p. 318.
[6]   A.K. Ghosh and C.H. Hamilton: Metall. Trans. A Vol. 10A (1979), p. 699.
[7]   R.S. Mishra, et al.: Mater. Sci. Eng. A Vol. A298 (2001), p. 44.
[8]   S.N. Patankar, et al.: J. Alloys and Compounds Vol. 345 (2002), p. 221.
[9]   G.A. Sargent, et al.: Metall. Mater. Trans. A Vol. 39A (2008), p. 2949.
[10] J.E. Bird, A.K. Mukherjee, and J.E. Dorn in: *Quantitative Relation between Microstructure and Properties*, edited by D.G. Brandon and A. Rosen, Israel Universities Press, Jerusalem, Israel (1969), p. 255.
[11] S.L. Semiatin, A.K. Ghosh, and J.J. Jonas: Metall. Trans. A Vol. 16A (1985), p. 2291.
[12] R.C. Gifkins: Metall. Trans. A Vol. 7A (1976), p. 1225.
[13] S.L. Semiatin, et al.: submitted to Metall. Mater. Trans. A (2009).
[14] S.L. Semiatin, N. Stefansson, and R.D. Doherty: Metall. Mater. Trans. A Vol. 36A (2005), p. 1372.
[15] S.L. Semiatin and J.J. Jonas: *Formability and Workability of Metals: Plastic Instability and Flow Localization* (American Society for Metals, Metals Park, OH 1984).